Progress In Electromagnetics Research C, Vol. 81, 21–30, 2018

Compact Dual-Wideband Bandpass Filter Using CSRR Based Extended Right/Left-Handed Transmission Line

Parya Fathi, Zahra Atlasbaf*, and Keyvan Forooraghi

Abstract—In this paper a miniaturized dual wideband bandpass filter is designed by the modified extended composite right/left-handed transmission line (ECRLH-TL) under balanced conditions in each right/left-hand passbands. A novel equivalent circuit is proposed to provide the design and an implementation of ECRLH unit-cell by means of the complementary, split ring resonator (CSRR) on the ground plane. Since CSRR is utilized as an alternative to implementing one of the resonators of ECRLH unit-cell, the size and complexity of the structure can be consequently reduced. An example of a dual band pass filter with 3 dB frequency bands from 3.2 to 4.8 GHz and from 6 to 7 GHz is investigated. There is a good agreement among circuit, electromagnetic simulations and measured results in both passbands. The measured insertion loss is better than 0.5 and 1 dB in first and second bands central frequency, respectively. The group delay which is an important factor in wideband communications is about 0.62 ns and 0.71 ns, respectively, in the first and second band central frequencies. The final dimensions of the miniaturized filter are reduced to 8.88 mm × 8.18 mm.

1. INTRODUCTION

In recent years, there has been great interest in wireless communication application operating at multiband frequencies, and miniaturization has become an important design issue. For this purpose, multiband filters play an important role in size reduction of devices used in multiband wireless telecommunication systems. Various methods have been introduced to design a dual band pass filter till now. A simple method is to use two band pass filters in the cascade, which increase the size of the filter and result in a bulky structure in microstrip [1]. Dual-mode dual-band filters were introduced later that use different resonating modes of a resonator to realize dual bands. Meander loop resonator [2], stepped impedance resonator [3, 4], and microstrip open loop resonator [5] are used as multi-mode resonators in this type of filters. Recently, metamaterial based composite right/left-handed (CRLH) transmission line has introduced a new method for designing and miniaturizing multiband microwave devices due to its unique phase response [6]. Moreover, CRLH transmission line is utilized in designing a single wideband bandpass filter [7–10]. For instance, in [11] and [12] an ultra-wideband bandpass filter is achieved by adopting the concept of balanced CRLH-TL to obtain a single band pass filter without any gap between right- and left-handed passbands. Extended composite right/left-handed (ECRLH) transmission lines are extended form of the CRLH transmission lines and can provide two wide bandpass frequency range under a balanced condition in each closed right/left-handed bands, so it can be utilized in designing dual wideband bandpass filters. The idea of such metamaterial transmission lines is proposed in [13] and [14] by combining the conventional CRLH (C-CRLH) and dual CRLH (D-CRLH) unitcell introduced in [15]. For the implementation of an ECRLH transmission line, various design procedures and layouts are proposed in different papers. In [16] a dual band pass filter is designed using a T model equivalent circuit and implemented in microstrip utilizing chip capacitors to realize capacitors in horizontal branch,

Received 2 October 2017, Accepted 14 January 2018, Scheduled 29 January 2018
* Corresponding author: Zahra Atlasbaf (atlasbaf@modares.ac.ir).
The authors are with the Faculty of Electrical and Computer Engineering, Tabriat Modares University, Tehran, Iran.

whereas in [17–19] a dual band pass filter is designed and implemented in a fully planar configuration by CPW, microstrip and SIW technology.

To decrease the size of the structure, recently defected ground structures (DGS) have been used in various shapes for filter applications [20, 21]. This paper proposes a CSRR based structure for the realization of an ECRLH transmission line to make a compact ECRLH unit cell which is utilized in the design of a dual wideband bandpass filter. The final results indicate that the group delay has good performance in both frequency bands which is required in wideband applications to keep the pulse distortion minimum. The paper is organized as follows. In Section 2, equivalent circuit and design procedure are discussed. Section 3 sheds light on the parameter extraction method utilized to get dimensions of each section. Section 4 presents the final layout of the filter. Simulated and measured results are compared in this section. Finally, in Section 4 the paper ends with conclusions.

2. DESIGN PROCEDURE

The equivalent circuit diagram and the proposed layout of a modified ECRLH unit-cell used here for realizing a dual band pass filter are shown in Fig. 1 and Fig. 2, respectively. It is derived from the modified Π equivalent circuit introduced in [22] with some extra modifications. The single C_{hp}/L_{hp} resonator of DCRLH part of the unit-cell in Fig. 1(a) is divided into two parts by $C/C_c/L_c$ resonator which models CSRR on the ground plane [23]. As will be presented in the next section, the advantage of the proposed circuit model is the reduction of the overall length of the cell since all resonators of the DCRLH part can be determined by CSRR on the ground plane and interdigital capacitor with a short narrow microstrip line on top of it which decreases the complexity of fabrication.

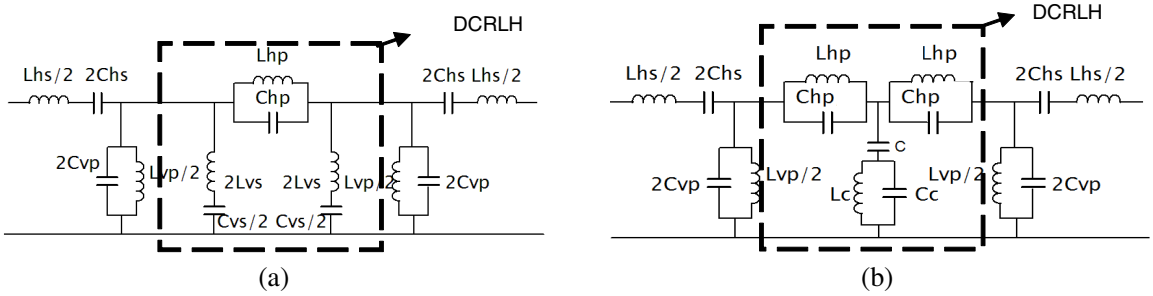

Figure 1. (a) Equivalent circuit for ECRLH-TL proposed in [22]. (b) Equivalent circuit for a modified ECRLH-TL realized by CSRR on the ground plane (Fig. 2).

In our previous paper [24], the same equivalent circuit is introduced with a distinct procedure to solve it for quad-band applications. However, in this work the equivalent circuit is solved for dual-band application using a different procedure for solving equations. At the first step, the modified Π equivalent circuit (Fig. 1(a)) is designed for the dual-band filter applications. By using the values obtained for elements L_{hs}, C_{hs}, L_{hp}, C_{hp}, C_{vp} and L_{vp} as initial values of the equivalent circuit elements in Fig. 1(b), in the second step our proposed equivalent circuit can be designed by means of optimization algorithms. At the beginning of optimization, arbitrary initial values can be chosen for elements C, C_c and L_c.

The Blotch analysis of the unit-cell depicted in Fig. 1(a) leads to the propagation constant and approximated Blotch impedance ($\beta d \ll 1$) as:

$$\beta d = \cos^{-1}(D) \tag{1}$$

$$Z_{bloch} = \sqrt{\frac{Z + Z_{hs}Z_{hp}Y}{Y}} = q \tag{2}$$

In which D is given in

$$D = 1 + 2ZY + 2Z_{hs}Z_{hp}Y^2 \tag{3}$$

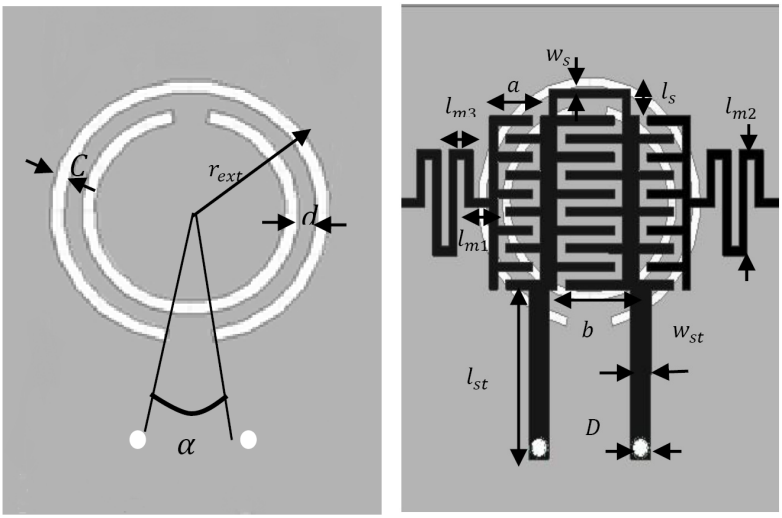

(a) (b)

Figure 2. The layout of dual-wideband bandpass filter. (a) Top view. (b) Bottom view. Dimensions are: a=1.07 mm, b=1.5 mm, l_s = 0.4 mm, w_s = 0.2 mm, w_{st} = 0.5 mm, α = 20°, l_{st} = 3.69 mm, l_{m1} = 0.5 mm, l_{m2} = 2.3 mm and l_{m3} = 0.6 mm. The width and separation of all interdigital capacitors are 0.2 mm, the width of meander line is 0.2 mm, the diameter of vias are 0.4 mm. For the CSRR the external radius is r_{ext} = 2.6 mm, the rings width are C = 0.2 mm and the separation between rings is d = 0.4 mm.

Z, Y, Z_{hs} and Y_{hp} are

$$\begin{aligned} Z &= \frac{1}{j\omega 2C_{hs}} + \frac{j\omega L_{hs}}{2} + \left(\frac{2}{j\omega L_{hp}} + j\omega 2C_{hp}\right)^{-1} \\ Y &= \frac{2}{j\omega L_{vp}} + j\omega 2C_{vp} + \left(\frac{2}{j\omega C_{vs}} + j\omega 2L_{vs}\right)^{-1} \\ Z_{hs} &= \frac{1}{j\omega 2C_{hs}} + \frac{j\omega L_{hs}}{2}, Z_{hp} = \left(\frac{2}{j\omega L_{hp}} + j\omega 2C_{hp}\right)^{-1}. \end{aligned} \tag{4}$$

By substituting q in the dispersion Equation (1), the following equation will be derived

$$Y^2(\omega) = \frac{1-\cos(\varphi)}{2q^2} = A^2 \tag{5}$$

in which A is a new parameter. It is desired to solve the above equation at four arbitrary frequencies, f_1, f_2, f_3 and f_4. To do this, the equation should be expanded and coefficients equated to the coefficients of

$$(\omega+\omega_4)(\omega-\omega_3)(\omega+\omega_2)(\omega-\omega_1) = 0 \tag{6}$$

Therefore, the first four elements' values can be easily obtained as follows

$$\begin{aligned} C_{vp} &= \frac{A}{2(\omega_4-\omega_3+\omega_2-\omega_1)} \\ L_{vp} &= \frac{2}{A}\left(\frac{1}{\omega_1} - \frac{1}{\omega_2} + \frac{1}{\omega_3} - \frac{1}{\omega_4}\right) \\ L_{vs} &= \frac{1}{4(a_1-\omega_{vp}^2-a_2)C_{vp}} \\ C_{vs} &= \frac{1}{a_2 L_{vs}} \end{aligned} \tag{7}$$

where a_1, a_2 and ω_{vp}^2 are

$$\begin{aligned} a_1 &= \omega_1\omega_2 - \omega_1\omega_3 + \omega_1\omega_4 + \omega_2\omega_3 - \omega_2\omega_4 + \omega_3\omega_4 \\ a_2 &= \frac{-\omega_1\omega_2\omega_3 + \omega_1\omega_2\omega_4 - \omega_1\omega_3\omega_4 + \omega_2\omega_3\omega_4}{\omega_4 - \omega_3 + \omega_2 - \omega_1} \\ \omega_{vp}^2 &= \frac{1}{L_{vp}C_{vp}}. \end{aligned} \tag{8}$$

Using $4C_{hs}L_{hp} = L_{vp}C_{vs}$ as a close stopped band condition the final four elements are obtained as

$$\begin{aligned} L_{hp} &= \frac{-L_{vp} + \sqrt{L_{vp}^2 + 4q^2C_{vs}L_{vp}}}{2} \\ C_{hp} &= \frac{1}{\omega_{hp}^2 L_{hp}} \\ C_{hs} &= \frac{C_{vs}L_{vp}}{4L_{hp}} \\ L_{hs} &= \frac{1}{\omega_{hs}^2 C_{hs}} \end{aligned} \tag{9}$$

where

$$\begin{aligned} \omega_{vs}^2 = \omega_{hp}^2 &= \frac{1}{L_{hp}C_{hp}} \\ \omega_{hs}^2 = \omega_{vp}^2 &= \frac{1}{L_{hs}C_{hs}} \end{aligned} \tag{10}$$

To design a dual band pass filter, at four cutoff band pass frequencies (f_1, f_2, f_3 and f_4), βd will equal $\pm\pi$, and the Blotch impedance will be set to the port impedance. By using eight equations, the circuit values will be calculated. Once the elements' values of the equivalent circuit in Fig. 1(a) are found, the initial elements' values of our proposed circuit are chosen by setting arbitrary initial values for elements C, C_c and L_c and equating other elements to the common elements' values derived by solving the equations. At the end, all elements' values will be optimized around their initial ones to obtain the final results.

In this work, two examples of dual wideband bandpass filter with the first 3 dB frequency band defined from 3.2 to 4.8 GHz and the second frequency band from 6 to 7 GHz are designed. Following the procedure discussed, the elements' values of the first equivalent circuit calculated for the port impedance of 50 Ω in the mentioned frequency ranges are: $L_{hs} = 4.8044$ nH, $C_{hs} = 0.259$ pF, $L_{vp} = 2.037$ nH, $C_{vp} = 0.612$ pF, $L_{hp} = 0.558$ nH, $C_{hp} = 1.428$ pF, $C_{vs} = 0.284$ pF, $L_{vs} = 2.803$ nH. After finding the initial common elements' values of our proposed equivalent circuit and setting arbitrary initial values for elements C, C_c and L_c, an optimization procedure in ADS is utilized to get the final elements' values as: $L_{hs} = 8.525$ nH, $C_{hs} = 0.145$ pF, $L_{vp} = 3.531$ nH, $C_{vp} = 0.221$ pF, $L_{hp} = 0.699$ nH, $C_{hp} = 1.154$ pF, $C = 0.5$ pF, $C_c = 1.770$ pF, $L_c = 0.345$ nH. To verify the design procedure, another filter is designed to operate at 2.2 to 3.6 GHz in the first band and 5 to 6 GHz in the second band. Final elements' values are presented in Table 1. Fig. 3 indicates the dispersion diagram and S parameters of these two filter design circuits simulated in ADS schematic part.

Table 1. Elements values of two filter design.

design	L_{hs} (nH)	C_{hs} (pF)	L_{vp} (nH)	C_{vp} (pF)	L_{hp} (nH)	C_{hp} (pF)	C (pF)	C_c (pF)	L_c (nH)
1	8.525	0.145	3.531	0.221	0.699	1.154	0.5	1.770	0.345
2	9	0.247	5.911	0.178	1.281	1.001	0.773	3.003	0.295

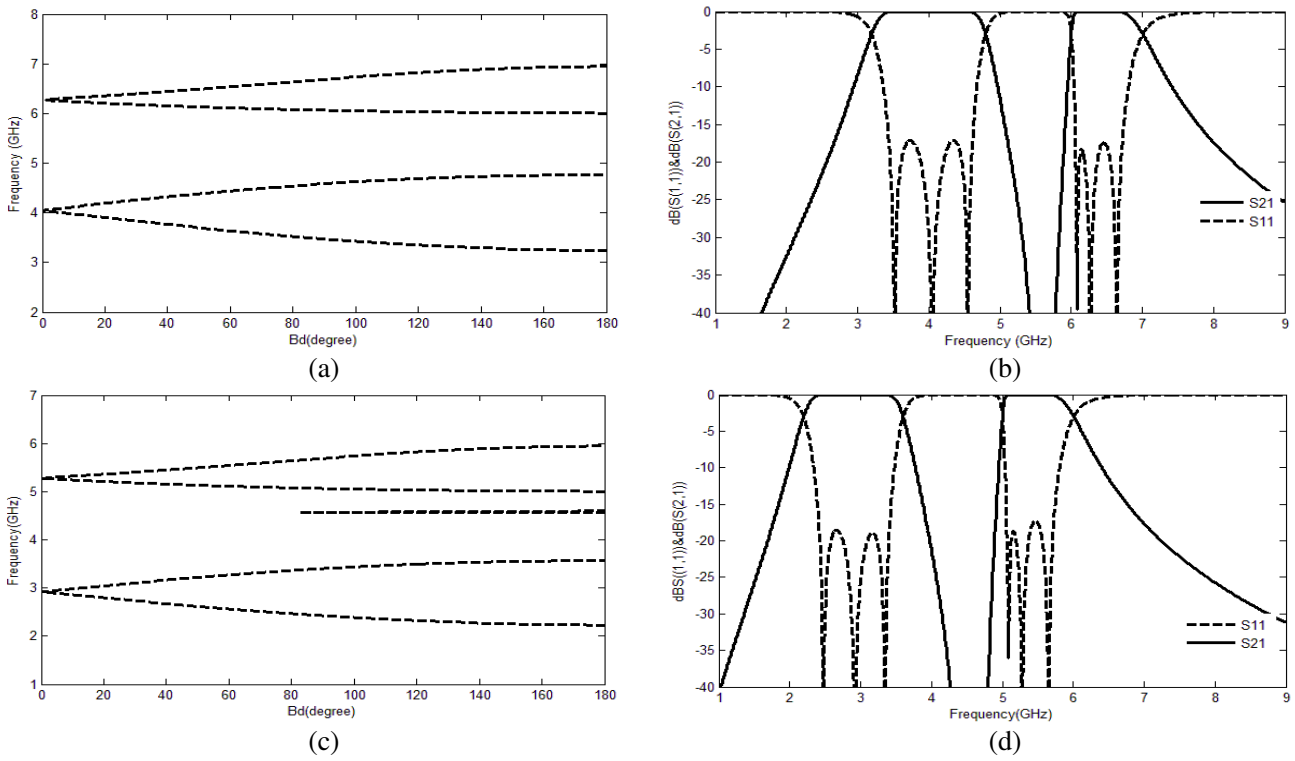

Figure 3. (a) Dispersion diagram of design 1. (b) S parameter of designed dual band filter of design 1. (c) Dispersion diagram of design 2. (d) S parameter of designed dual band filter of design 2.

3. PARAMETER EXTRACTION

The structure of the proposed layout depicted in Fig. 2 is designed on a substrate of Rogers4003 with thickness $h = 1.524\,\text{mm}$ and electric constant $\varepsilon_r = 3.55$. L_{hp} and C_{hp} are realized by an interdigital capacitor with a narrow strip. L_{hs} and C_{hs} are implemented by a meander inducer and an interdigital capacitor. L_{vp} and C_{vp} are achieved by a stub connected to the ground by vias, and CSRR etched on the ground plane realizes C, C_c and L_c. To find the dimensions of the layout, each part is simulated individually in HFSS, and their parameters are extracted using the method in [25] for CSRR and the procedure introduced in [26] for other parts.

3.1. Interdigital Capacitor

Neglecting the parasitic elements of an interdigital capacitor, its main capacitance can be easily calculated from the following equation using Y parameters. Fig. 4 shows how the digits width and length affect the final value of the capacitance. Undoubtedly, the capacitance value varies with frequency, and less variation leads to more accurate results.

$$C_s = \frac{2}{j\omega} \frac{1}{\left(\omega \dfrac{\partial\left(1/Y_{12}\right)}{\partial\omega} - \dfrac{1}{Y_{12}}\right)} \tag{11}$$

3.2. Stub Inducer

The inductance and capacitance of a stub connected to ground can be easily extracted utilizing Z parameters from the equations below. Fig. 5 shows the various values of inductance and capacitance

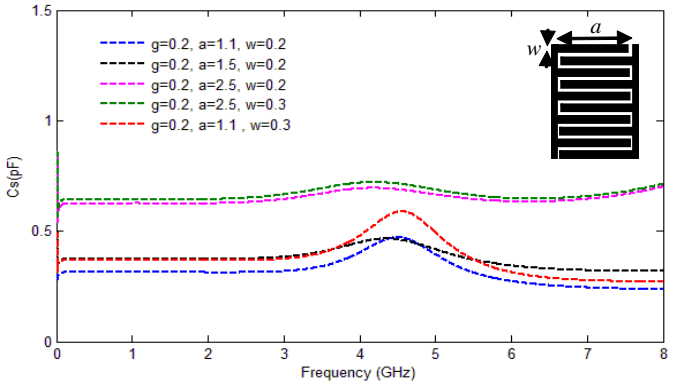

Figure 4. Interdigital capacitance values extracted using the parameter extraction method. (g is the space between digits of capacitance).

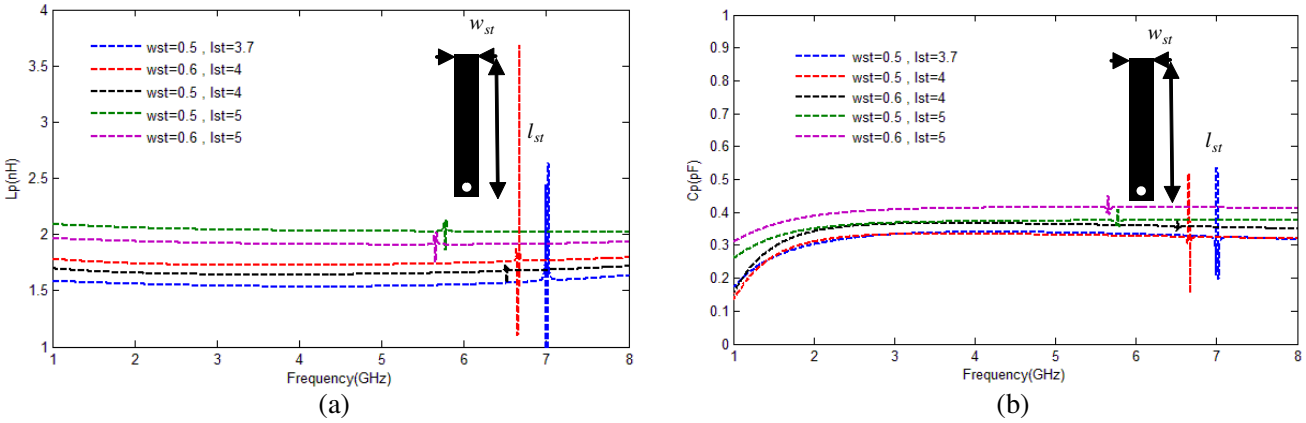

Figure 5. (a) Inductance, (b) capacitance of stub extracted using the parameter extraction method with different width and length.

extracted in various lengths and widths.

$$C_p = \frac{1}{2j\omega}\left(\omega\frac{\partial(1/Z_{12})}{\partial\omega} + \frac{1}{Z_{12}}\right)$$
$$L_p = \frac{2j}{\omega}\frac{1}{\left(\omega\frac{\partial(1/Z_{12})}{\partial\omega} - \frac{1}{Z_{12}}\right)} \tag{12}$$

3.3. Meander Line

Meander lines usually are utilized when there is a need for big inductance with less space for implementation. The inductance of meander line can also be extracted from Y parameters using the equation below. We neglect the parasitic element due to its small value. Fig. 6 indicates the extracted inductance for various lengths and widths of the meander line.

$$L_s = \frac{2}{j\omega}\frac{1}{\left(Y_{11} - \omega\frac{\partial Y_{11}}{\partial\omega}\right)} \tag{13}$$

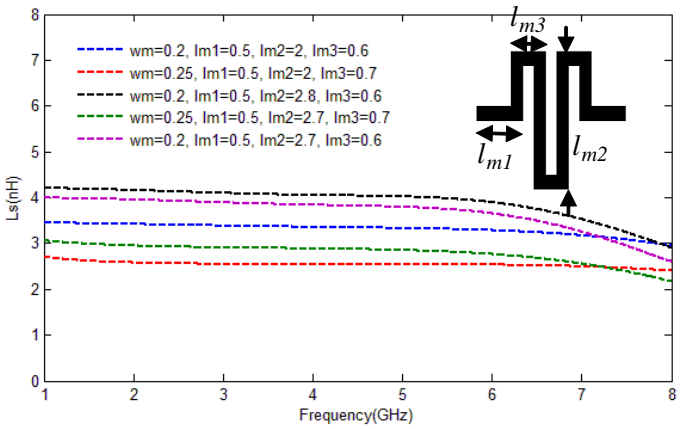

Figure 6. Inductance of meander line extracted using the parameter extraction method with different width and length.

4. FABRICATION RESULTS

All dimensions of the tentative layout are calculated separately, and finally, after accumulating all elements, an optimization is done to obtain the final values. The optimization procedure includes two steps. The first step is to tune the resonators' dimensions in predefined ranges and compare the frequency response to that of electrical circuit. When the approximate dimensions of the layout are found, the final dimensions that best fit the requirements will be achieved using the optimization tool in HFSS.

The frequency responses of filter obtained from measurements, electromagnetic, and circuit simulations are depicted in Fig. 7. The discrepancies in the S_{11} parameter between the circuit and electromagnetic simulations are related to parasitic elements omitted in circuit simulation for simplicity. Totally good agreement between EM simulations and measurements is observed, and the slight degradations are due to fabrication tolerance. Return loss larger than 16.5 dB and insertion loss less than 0.5 dB with FBW of 40% are achieved at the first passband center frequency of 4 GHz. Similarly, the measured return loss, insertion loss, and FBW at the second passband center frequency of 6.5 GHz are given as 15.6 dB, 0.9 dB, and 15.38%, respectively. Furthermore, the group delay of the filter is illustrated in Fig. 8. It is about 0.62 ns and 0.71 ns in centers of the first and second bands, respectively, and almost constant in both bands. A photographs of the fabricated dual-band filter is shown in Fig. 9. The filter size excluding the feed lines is 8.88 mm × 8.18 mm. The filter's dimensions are decreased in comparison to pervious works. In Table 2, the results are compared with other works in details.

Table 2. Performance comparison of the proposed filter with previous works.

References	Substrate H (mm)/ε_r	Dual center freq (GHz)	Insertion loss (dB)	3 dB FBW (%)	Circuit size (mm × mm)
[2]	0.508/3.5	2.71/5.14	0.57/0.73	42.8/20.8	10.31 × 10.31
[3]	1.6/ 4.5	2.4/3.8	0/ 0.5	8.33/5.26	20 × 30
[6]	0.787/2.2	2.4/5.2	0.21/0.5	33.8/38.4	18.8 × 35.2
[17]	1.27/1.96	4.1/5.6	1/1.5 <	23/23	14.3 × 28.34
This work	1.524 / 3.55	4 / 6.5	0.4 / 0.9	40/15.38	8.88 × 8.18

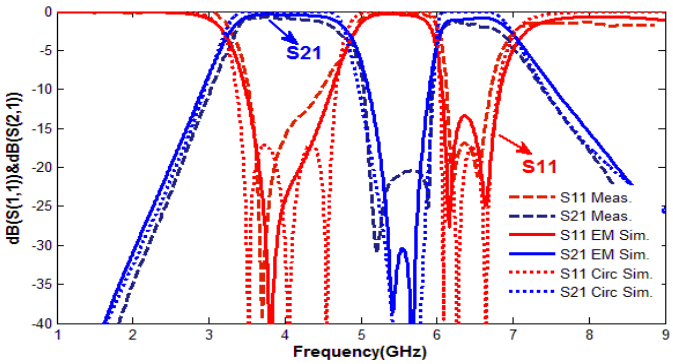

Figure 7. The frequency response of dual band filter. The measurements show that the filter operates in the frequency band from 3.2 to 4.8 GHz and from 6 to 7 GHz.

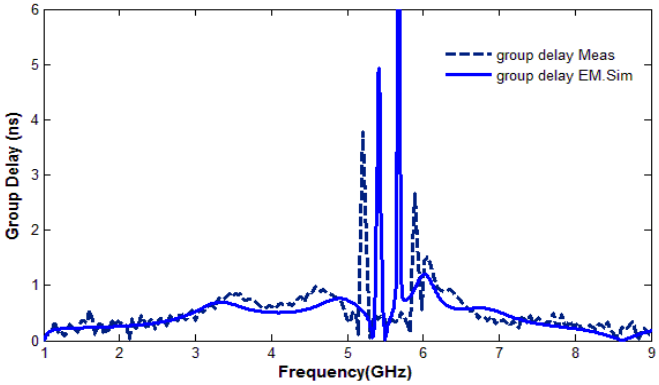

Figure 8. Group delay of dual band filter inferred from measurements and electromagnetic simulation.

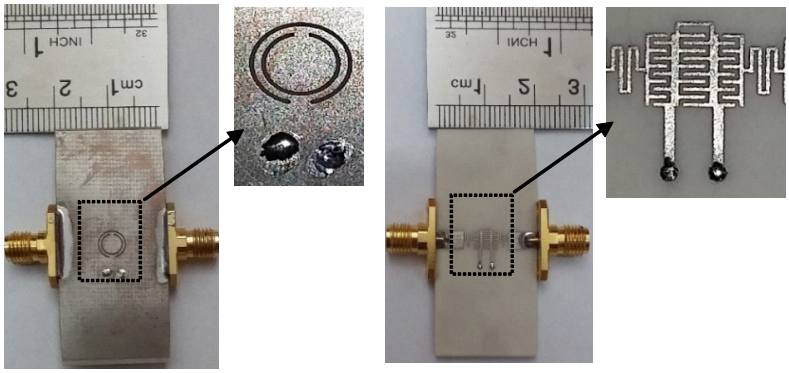

Figure 9. Photograph of fabricated dual band filter.

5. CONCLUSIONS

In this paper, a novel dual wideband bandpass filter is designed, simulated and measured based on CSRR loaded on the ground plane, resulting in size reduction of the structure. The equivalent circuit is derived, and the elements' values are calculated for dual-band applications using an optimization method. The first tentative layout's dimensions are obtained by means of parameter extraction, and lastly an optimization is done to get final dimensions. The advantages of the proposed filter are its wide bandwidth in both frequency bands, reduction of its size and complexity, and fully planar implementation.

REFERENCES

1. Liu, Y. and W. Dou, "A dual-band filter realized by alternately connecting the main transmission-line with shunt stubs and shunt serial resonators," *IEEE Microw. Wirel. Components Lett.*, Vol. 19, No. 5, 296–298, 2009.
2. Li, X., Y. Zhang, J. Xie, X. Zhang, Y. Tian, and Y. Fan, "Dual band bandpass filter using meander split loop resonator," *Microw. Opt. Technol. Lett.*, Vol. 59, No. 10, 2490–2493, 2017.
3. Kim, C., T. Hyeon Lee, B. Shrestha, and K. Chul Son, "Miniaturized dual-band bandpass filter based on stepped impedance resonators," *Microw. Opt. Technol. Lett.*, Vol. 59, No. 5, 1116–1119, 2017.
4. Firmansyah, T., S. Praptodinoyo, R. Wiryadinata, S. Suhendar, S. Wardoyo, A. Alimuddin, C. Chairunissa, M. Alaydrus, and G. Wibisono, "Dual-wideband band pass filter using folded cross-stub stepped impedance resonator," *Microw. Opt. Technol. Lett.*, Vol. 59, No. 11, 2929–2934, 2017.
5. Feng, W., Y. Zhang, and W. Che, "Tunable dual-band filter and diplexer based on folded open loop ring resonators," *IEEE Trans. Circuits Syst. II Express Briefs*, Vol. 64, No. 9, 1047–1051, 2017.
6. An, B., G. Chaudhary, and Y. Jeong, "Size reduction of composite right/left handed transmission line and its application to the design of dual-band bandpass filter," *Microw. Opt. Technol. Lett.*, Vol. 59, No. 9, 2272–2276, 2017.
7. Eleftheriades, G. V., A. K. Iyer, and P. C. Kremer, "Planar negative refractive index media using periodically LC loaded transmission lines," *IEEE Trans. Microw. Theory Tech.*, Vol. 50, No. 12, 2702–2712, 2002.
8. Caloz, C., A. Sanada, and T. Itoh, "Microwave circuits based on negative refractive index material structures," *33rd Eur. Microw. Conf. 2003*, No. c, 2003.
9. Norooziarab, M., Z. Atlasbaf, and F. Farzami, "Substrate integrated waveguide loaded by 3-dimensional embedded split ring resonators," *AEU-International J. Electron. Commun.*, Vol. 68, No. 7, 658–660, 2014.
10. Keshavarzi, S. and Z. Atlasbaf, "Switchable bandpass filter using CRLH cells based on a new kind of admittance inverter," *Int. J. Microw. Wirel. Technol.*, Vol. 9, No. 1, 61–69, 2017.
11. Kahng, S. and J. Ju, "Design of the UWB bandpass filter based on the 1 cell of microstrip CRLH-TL," *2008 Int. Conf. Microw. Millim. Wave Technol. Proceedings, ICMMT*, Vol. 1, 69–72, 2008.
12. Huang, J.-Q. and Q.-X. Chu, "Compact UWB band-pass filter utilizing modified composite right/left-handed structure with cross coupling," *Progress In Electromagnetics Research*, Vol. 107, 179–186, 2010.
13. Rennings, A., S. Otto, J. Mosig, C. Caloz, and I. Wolff, "Extended composite right/left-handed (E-CRLH) metamaterial and its application as quadband quarter-wavelength transmission line," *Microwave Conference, 2006. APMC 2006. Asia-Pacific*, 2006, 1405–1408.
14. Eleftheriades, G. V. and A. Abstract, "A generalized negative-refractive-index transmission-line (NRI-TL) metamaterial for dual-band and quad-band applications," *Microw. Wirel. Components Lett. IEEE*, Vol. 17, No. 6, 415–417, 2007.
15. Caloz, C., "Dual composite right/left-handed (D-CRLH) transmission line metamaterial," *IEEE Microw. Wirel. Components Lett.*, Vol. 16, No. 11, 585–587, 2006.
16. Studniberg, M. and G. V. Eleftheriades, "A dual-band bandpass filter based on generalized negative-refractive-index transmission-lines," *IEEE Microw. Wirel. Components Lett.*, Vol. 19, No. 1, 2009–2011, 2009.
17. Duran-Sindreu, M., J. Bonache, and F. Martin, "Compact CPW dual-band bandpass filters based on semi-lumped elements and metamaterial concepts," *2010 Asia-Pacific Microw. Conf.*, Vol. 1, No. c, 670–673, 2010.
18. Duran-Sindreu, M., G. Siso, J. Bonache, and F. Martin, "Planar multi-band microwave components based on the generalized composite right/left handed transmission line concept," *IEEE Trans. Microw. Theory Tech.*, Vol. 58, No. 12, Part 2, 3882–3891, 2010.

19. Duran-Sindreu, M., J. Bonache, F. Martin, T. Itoh, P. B. Structures, and P. Components, "Single-layer fully-planar extended-composite right-/left-handed transmission lines based on substrate integrated waveguides for dual-band and quad-band applications," *Int. J. Microw. Wirel. Technol.*, Vol. 5, No. 03, 213–220, 2013.
20. Boutejdar, A., M. Challal, A. Omar, E. Burte, R. Mikuta, and A. Azrar, "A novel band-stop filter using octagonal-shaped patterned ground structures along with interdigital and compensated capacitors," *ACES Journal — The Appl. Comput. Electromagn. Issue*, Vol. 26, No. 10, 2011.
21. Boutejdar, A., A. Omar, and E. Burte, "High-performance wide stop band low-pass filter using a vertically coupled DGS-DMS-resonators and interdigital capacitor," *Microw. Opt. Technol. Lett.*, Vol. 56, No. 1, 87–91, 2014.
22. Ryan, C. G. M. and G. V. Eleftheriades, "Design of a printed dual-band coupled-line coupler with generalised negative-refractive index transmission lines," *IET Microwaves, Antennas Propag.*, Vol. 6, No. 6, 705, 2012.
23. Marqués, R., F. Martín, and M. Sorolla, *Metamaterials with Negative Parameters: Theory, Design and Microwave Applications*, Vol. 183. John Wiley & Sons, 2011.
24. Fathi, P., Z. Atlasbaf, and K. Forooraghi, "Modified extended composite right/left-handed layout loaded with CSRR for quad band applications," *Progress In Electromagnetics Research Letters*, Vol. 61, 7–12, 2016.
25. Bonache, J., M. Gil, I. Gil, J. Garcia-Garcia, and F. Martin, "On the electrical characteristics of complementary metamaterial resonators," *IEEE Microw. Wirel. Components Lett.*, Vol. 16, No. 10, 543–545, 2006.
26. Caloz, C. and T. Itoh, *Electromagnetic Metamaterials: Transmission Line Theory and Microwave Applications*, John Wiley & Sons, 2005.